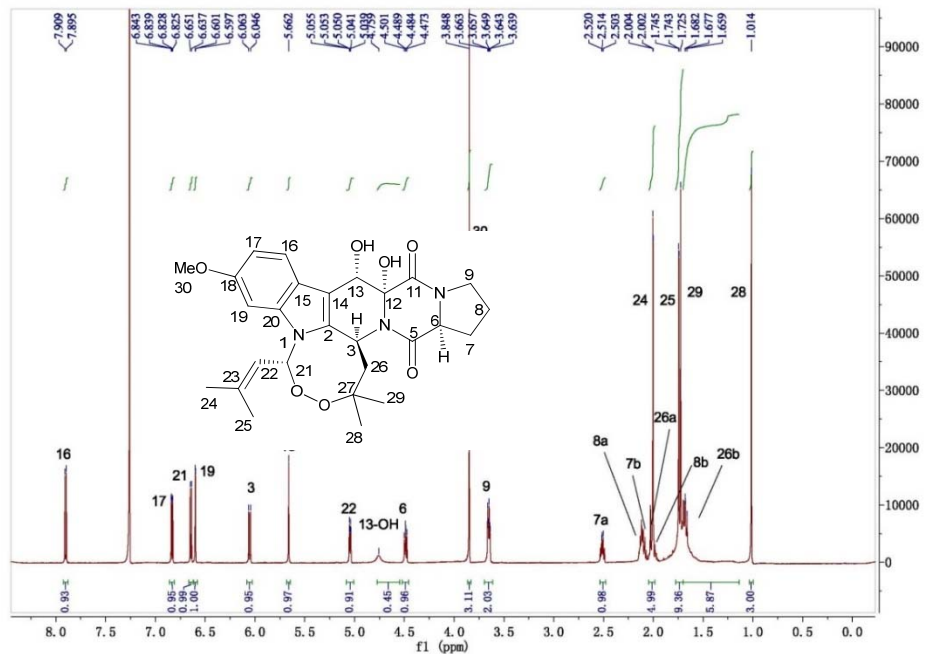


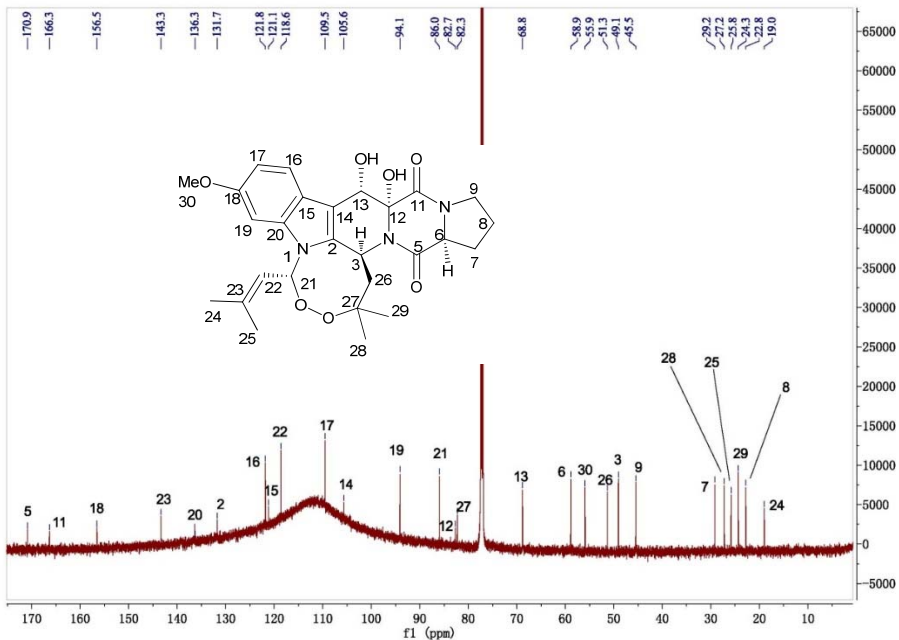
Supplementary Information:

Chemical Characterization:

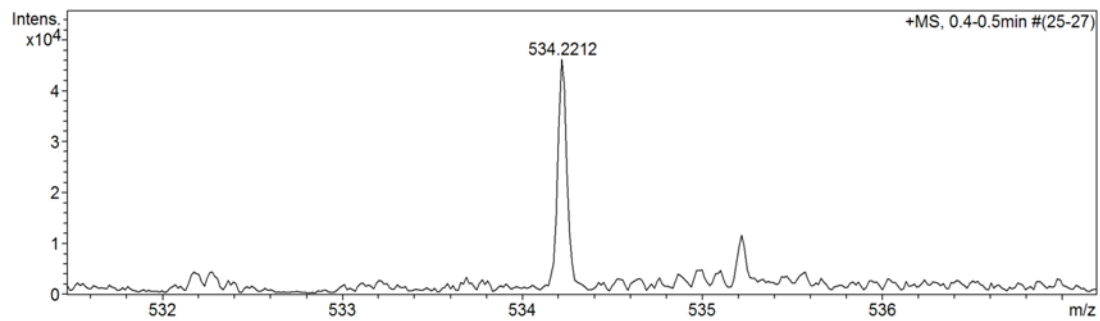
1. ^1H -NMR, ^{13}C -NMR and high-resolution mass spectrometry characterization of verruculogen (**2**)



¹H NMR (600 MHz, CDCl₃) spectrum of verruculogen (**2**) in CDCl₃.

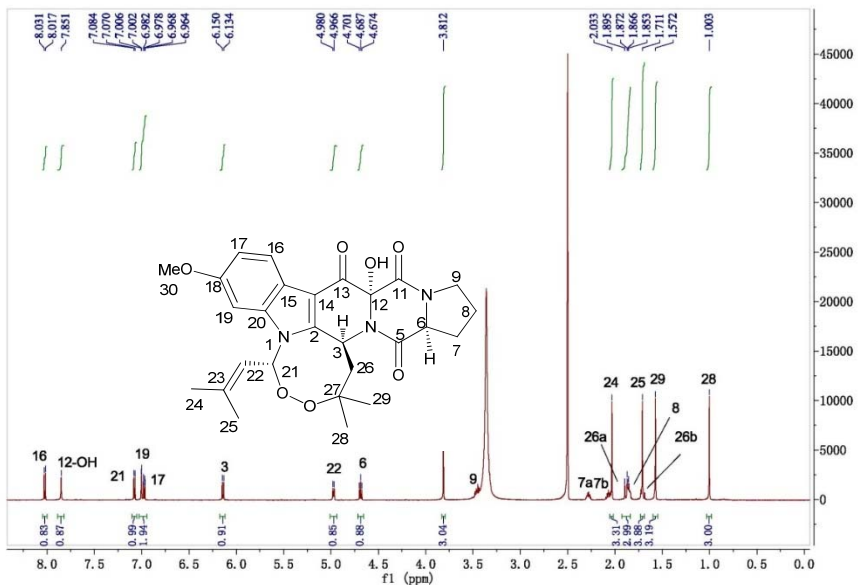


¹³C NMR (150 MHz, CDCl₃) spectrum of verruculogen (**2**) in CDCl₃.

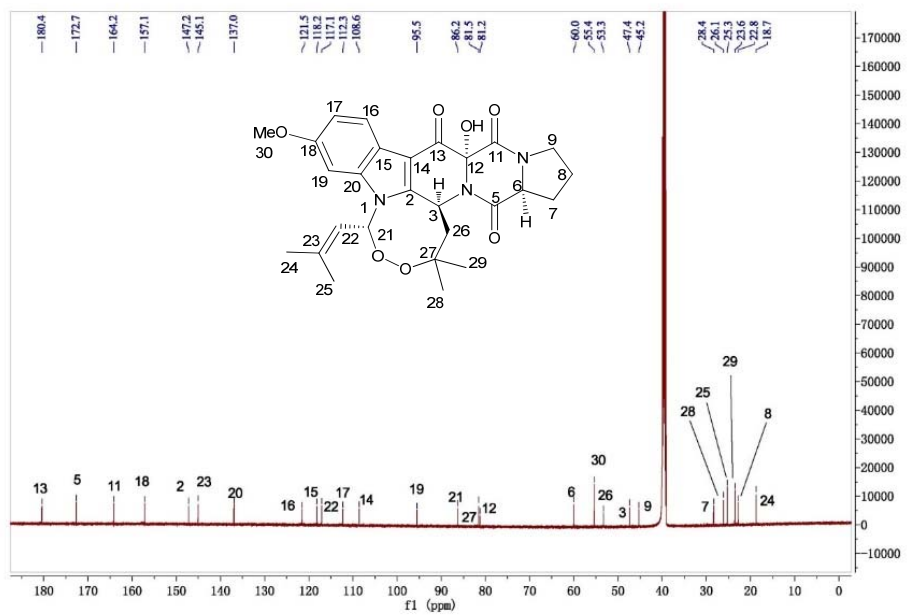


Molecular ion region in the high resolution ESI mass spectrum of verruculogen (**2**) (detected at m/z 534.2212, calculated for $C_{27}H_{33}N_3O_7Na$: m/z 534.2211).

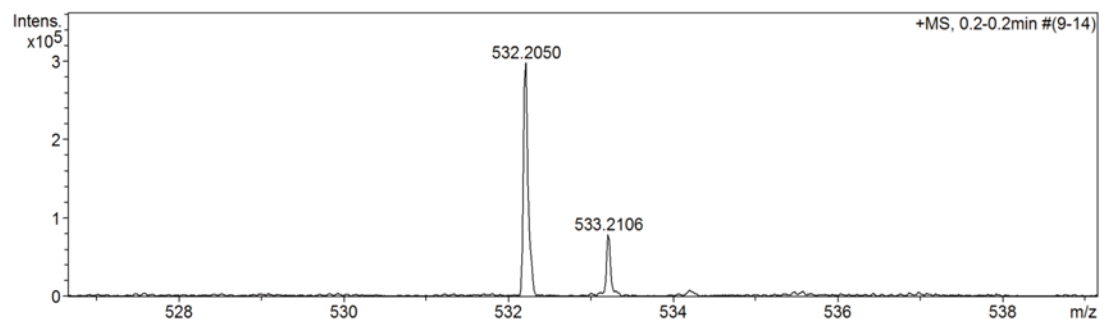
2. 1H -NMR, ^{13}C -NMR and high-resolution mass spectrometry Characterization of 13-oxoverruculogen (**3**).



1H NMR (600 MHz, DMSO- d_6) spectrum of 13-oxoverruculogen (**3**).



^{13}C NMR (150 MHz, DMSO- d_6) spectrum of 13-oxoverruculogen (**3**).

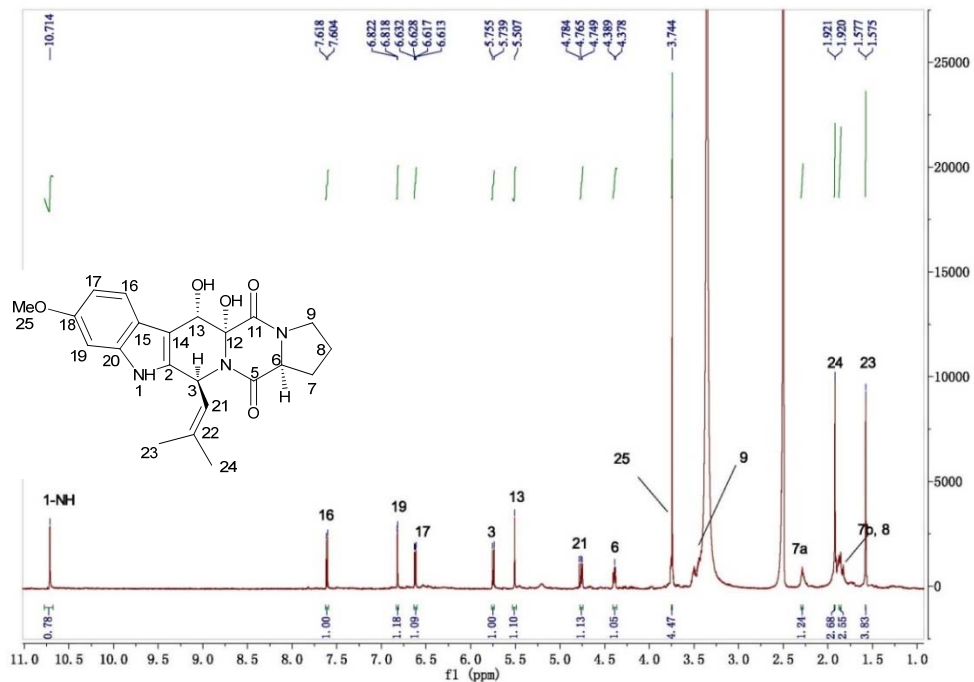


Molecular ion region in the high resolution ESI mass spectrum of 13-oxoverruculogen (**3**) (detected at m/z 532.2050, calculated for $\text{C}_{27}\text{H}_{31}\text{N}_3\text{O}_7\text{Na}$: m/z 532.2054).

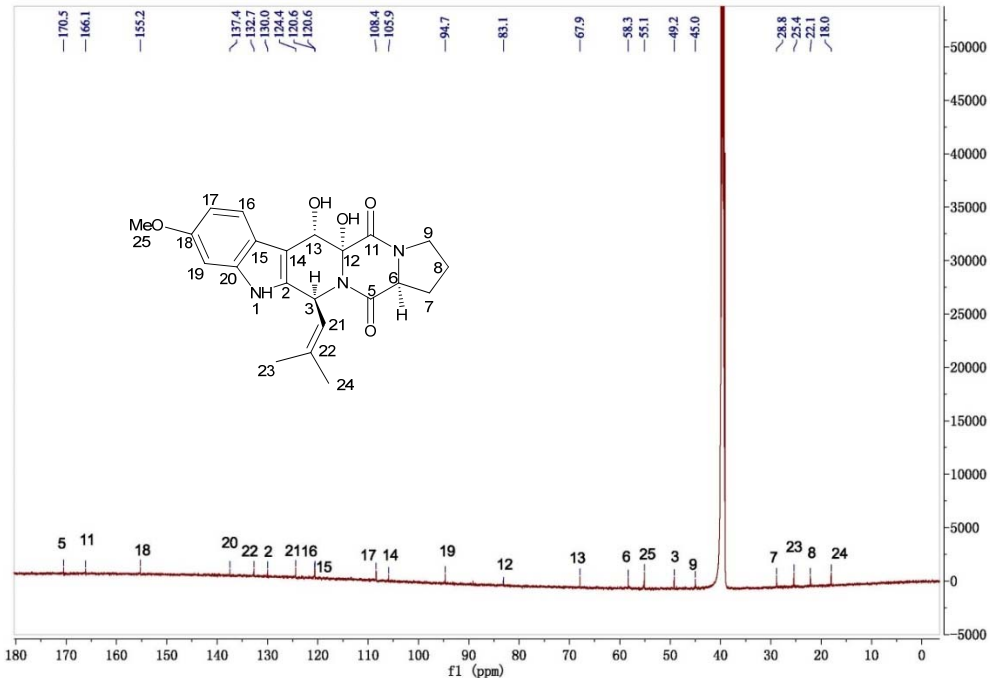
Summary of the chemical shifts and coupling constants for 13-oxoverruculogen (**3**) and verruculogen (**2**) (NMR, 600 MHz).

pos	13-oxoverruculogen in DMSO- <i>d</i> ₆		verruculogen in CDCl ₃	
	δ _H , mult (J in Hz)	δ _C	δ _H , mult (J in Hz)	δ _C
2		147.2		131.7
3	6.14, d (9.6)	47.4	6.06, d (10.2)	49.1
5		172.7		170.9
6	4.69, t (7.8)	60.0	4.48, dd (9.6, 7.2)	58.9
7a	2.28, m	28.4	2.51, m	29.2
7b	2.07, m		2.11, overlap	
8a	1.86 m	22.8	2.12, overlap	22.8
8b			1.98, m	
9a	3.45, m	45.2	3.65, m	45.5
9b	3.33, m			
11		164.2		166.3
12		81.2		82.7
13		180.4	5.66, s	68.8
14		108.6		105.6
15		118.2		121.1
16	8.02 d (8.4)	121.5	7.90, d (8.4)	121.8
17	6.97, dd (8.4, 2.4)	112.3	6.83, dd (8.4, 2.4)	109.5
18		157.1		156.5
19	7.00, d (2.4)	95.5	6.60, d (2.4)	94.1
20		137.0		136.3
21	7.08, d (8.4)	86.2	6.64, d (8.4)	86.0
22	4.97, brd (8.4, 1.2, 1.2)	117.1	5.05, dqq (8.4, 1.2, 1.2)	118.6
23		145.1		143.3
24	2.03, s	18.7	2.00, d (1.2)	19.0
25	1.71, s	25.3	1.74, d (1.2)	25.8
26a	1.87, overlap	53.3	2.01, d (13.2)	51.3
26b	1.71, overlap		1.68, dd (13.2, 10.2)	
27		81.5		82.3
28	1.00, s	26.1	1.01, s	27.2
29	1.57, s	23.6	1.72, s	24.3
30	3.81, s	55.4	3.85, s	55.9
12-OH	7.85, s			
13-OH			4.76, s	

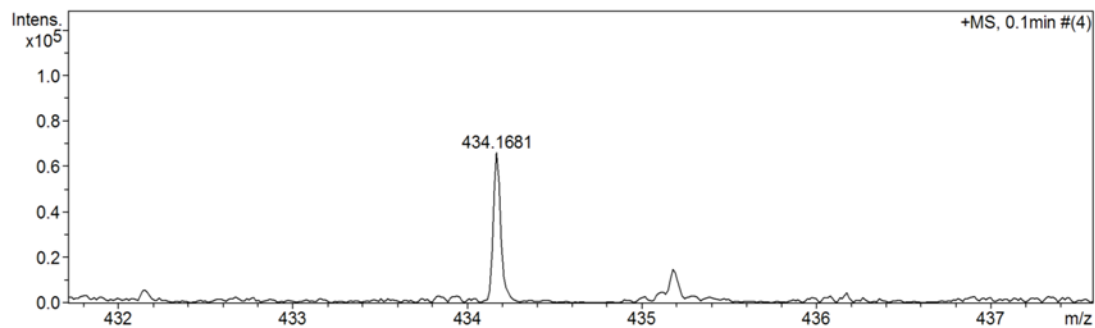
3. ^1H -NMR, ^{13}C -NMR and high-resolution mass spectrometry characterization of 12,13-dihydroxy-fumitremorgin C (4**),**



^1H NMR (600 MHz, DMSO- d_6) spectrum of 12,13-dihydroxy-fumitremorgin C (**4**).

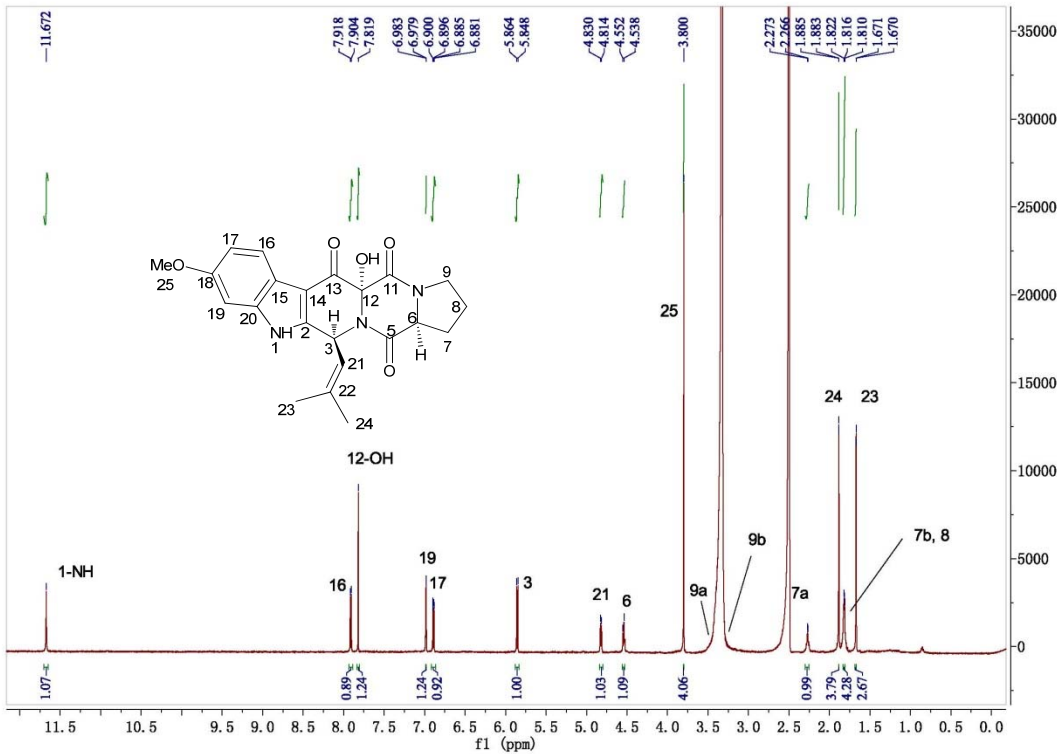


^{13}C NMR (150 MHz, DMSO- d_6) spectrum of 12,13-dihydroxy-fumitremorgin C (**4**).

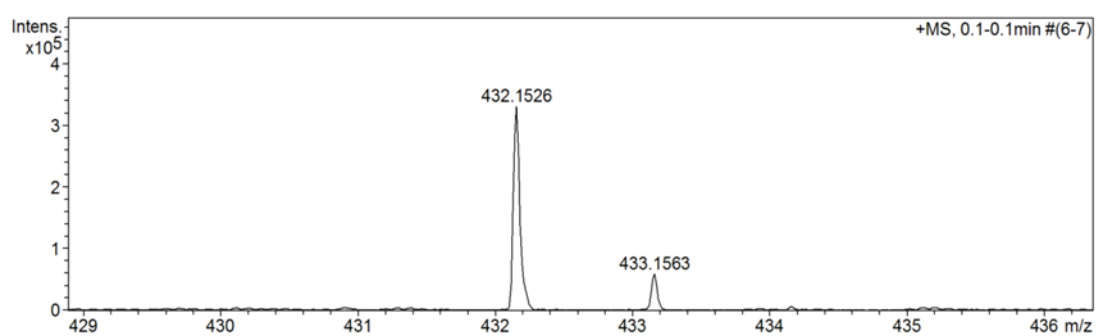
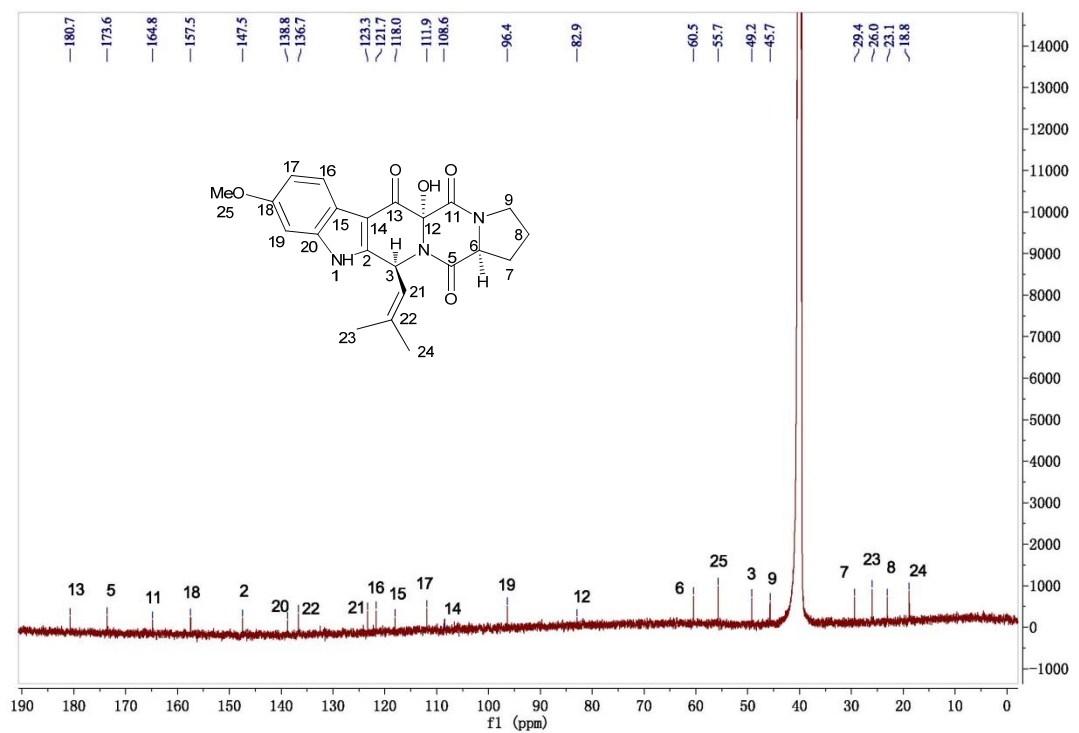


Molecular ion region in the high resolution ESI mass spectrum of 12,13-dihydroxy-fumitremorgin C (**4**) (detected at m/z 434.1681, calculated for $C_{22}H_{25}N_3O_5Na$: m/z 434.1692).

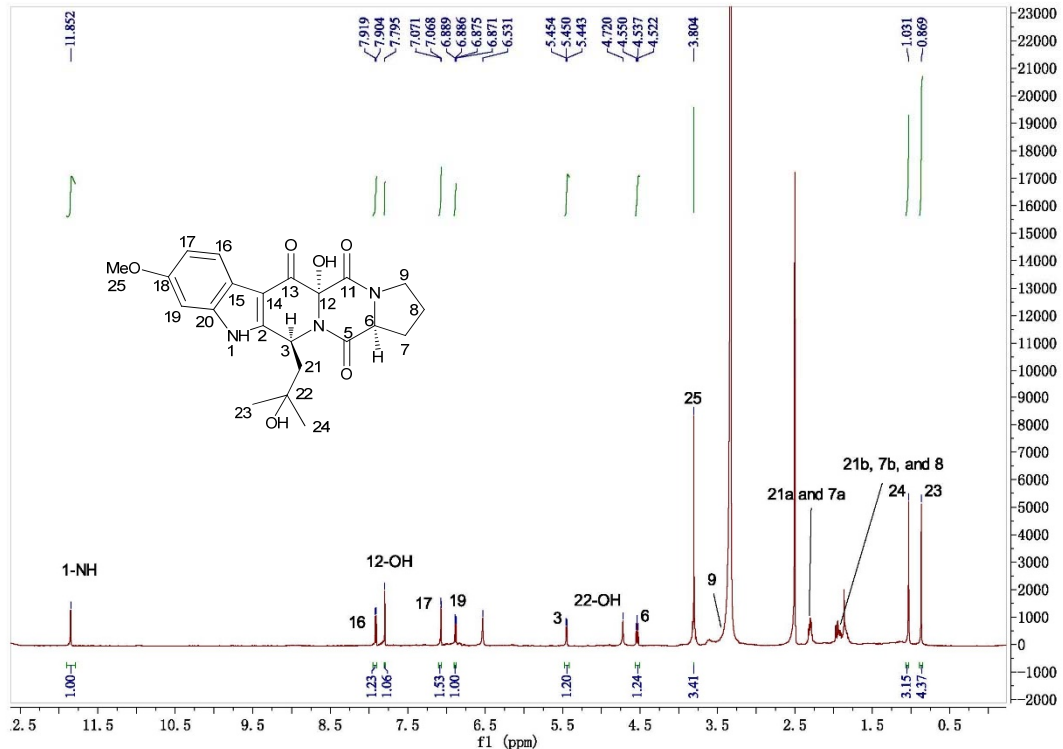
4. 1H -NMR, ^{13}C -NMR and high-resolution mass spectrometry characterization of 12-hydroxy-13-oxofumitremorgin C (**5**).



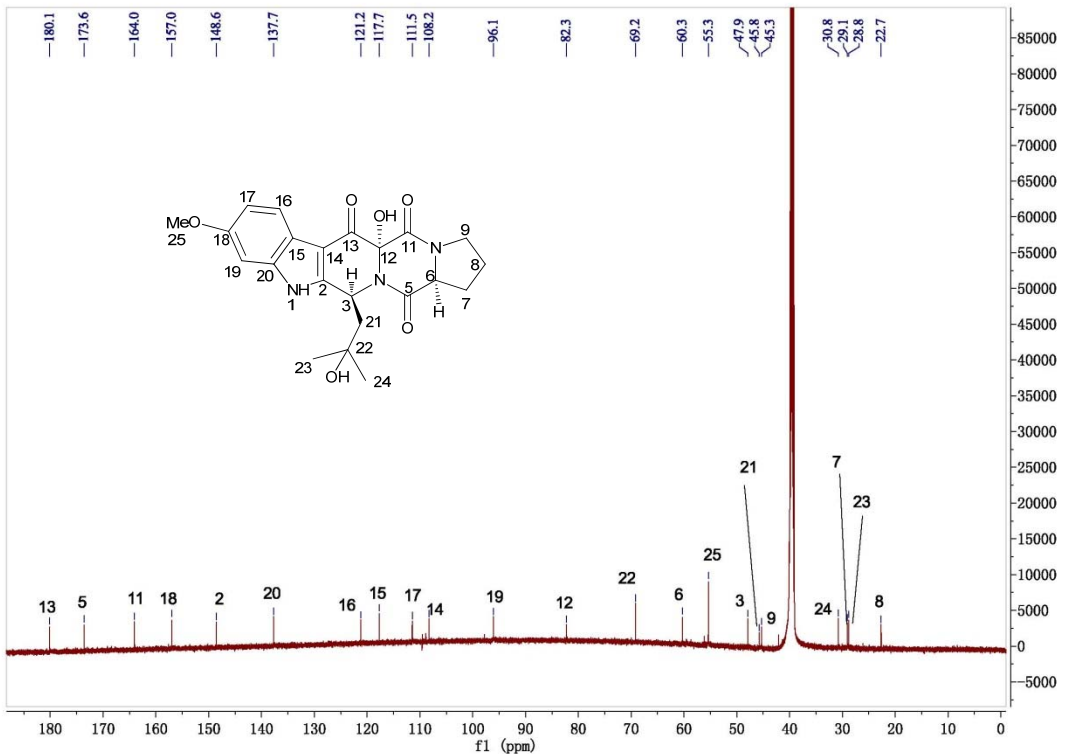
1H NMR (600 MHz, DMSO-*d*₆) spectrum of 12-hydroxy-13-oxofumitremorgin C (**5**).



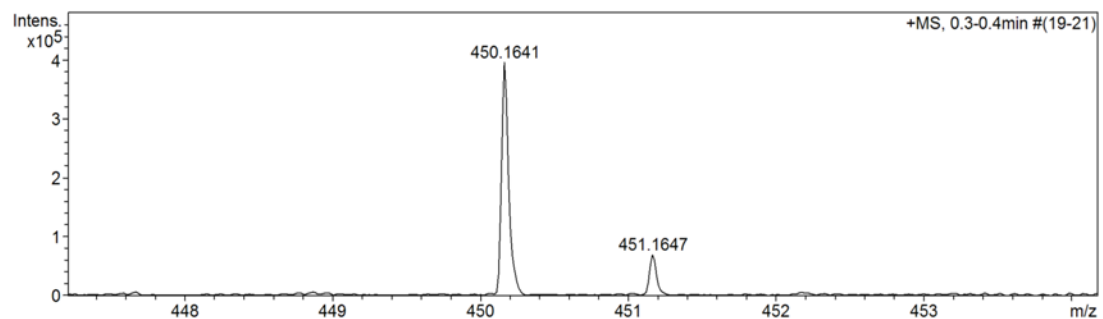
¹H-NMR, ¹³C-NMR and high-resolution mass spectrometry characterization of 12,22-dihydroxy-13-oxofumitremorgin C (**6**).



¹H NMR (600 MHz, DMSO-*d*₆) spectrum of 12,22-dihydroxy-13-oxofumitremorgin C (**6**).



¹³C NMR (150 MHz, DMSO-*d*₆) spectrum of (3*S*) -12,22-dihydroxy-13-oxofumitremorgin C (**6**).



Molecular ion region in the high resolution ESI mass spectrum (*3S*)-12,22-dihydroxy-13-oxofumitremorgin C (**6**) (detected at m/z 450.1641, calculated for $C_{22}H_{25}N_3O_6Na$, m/z 450.1636).

Summary of the chemical shifts and coupling constants for 12,13-dihydroxy-fumitremorgin C (**4**), 12-hydroxy-13-oxofumitremorgin C (**5**), and (3*S*)-12,22-dihydroxy-13-oxofumitremorgin C (**6**) (NMR, 600 MHz).

pos	5		4	
	δ_{H} mult (J in Hz)	δ_{C}	δ_{H} mult (J in Hz)	δ_{C}
2		147.5		130.0
3	5.86, d (9.0)	49.2	5.75, d (9.0)	49.2
5		173.6		170.5
6	4.54, dd (7.8, 7.2)	60.5	4.39, dd (9.6, 7.2)	58.3
7a	2.28, m	29.4	2.28, m	28.8
7b	1.82, overlap		1.86, overlap	
8	1.82, overlap	23.1	1.89, overlap	22.1
9a	3.41, overlap	45.7	3.50, overlap	45.0
9b	3.32, overlap		3.45, overlap	
11		164.8		166.1
12		82.9		83.1
13		180.7	5.51, s	67.9
14		108.6		105.9
15		118.0		120.6
16	7.91, d (8.4)	121.7	7.61, d (8.4)	120.6
17	6.89, dd (8.4, 2.4)	111.9	6.62, dd (8.4, 2.4)	108.4
18		157.5		155.2
19	6.98, d (2.4)	96.4	6.82, d (2.4)	94.7
20		138.8		137.4
21	4.82, dq (9.0, 1.2)	123.3	4.76, dq (9.0, 1.2)	124.4
22		136.7		132.7
23	1.67, d (1.2)	26.0	1.58, d (1.2)	25.4
24	1.88, d (1.2)	18.8	1.92, d (1.2)	18.0
25	3.80, s	55.7	3.74, s	55.1
12-OH	7.82, s			
1-NH	11.67, s		10.71, s	

pos	6	
	δ_{H} mult (J in Hz)	δ_{C}
2		148.6
3	5.45, dd (6.0, 1.8)	47.9
5		173.6
6	4.54, t (9.0)	60.3
7a	2.29, overlap	29.1
7b	1.93, overlap	
8	1.85, overlap	22.7
9	3.34, overlap	45.3
11		164.0
12		82.3
13		180.1
14		108.2
15		117.7
16	7.91, d (8.4)	121.2
17	6.88, dd (8.4, 2.4)	111.5
18		157.0
19	7.10, d (2.4)	96.1
20		137.7
21a	2.31, overlap	45.8
21b	1.96, overlap	
22		69.2
23	1.03, s	28.8
24	0.87, s	30.8
25	3.80, s	55.3
12-OH	7.80, s	
1-NH	11.85, s	

Videos: Movies of FtmOx1 and TauD active sites. Two separate movies are loaded as online supporting information to show the active site binding mode differences. In FtmOx1 movie, the water molecule is blocked from substrate access by Y224. This is in contrast to the active site in TauD, in which the water molecule faces directly to the substrate binding pocket.